J Vet Intern Med 2011;25:1036–1043

Assessment of Global and Regional Left Ventricular Volume and Shape by Real-Time 3-Dimensional Echocardiography in Dogs with Myxomatous Mitral Valve Disease

I. Ljungvall, K. Höglund, C. Carnabuci, A. Tidholm, and J. Häggström

Background: Left ventricular (LV) remodeling occurs in response to chronic volume overload. Real-time 3-dimensional (RT3D) echocardiography offers new modalities for LV assessment.

Objective: To investigate LV changes in shape and volume in response to different severities of naturally acquired myxomatous mitral valve disease (MMVD) in dogs by RT3D echocardiography.

Animals: Sixty-five client-owned dogs.

Methods: Prospectively recruited dogs were classified by standard echocardiography into healthy, mild, moderate, and severe MMVD groups. Endocardial border tracking of LV RT3D dataset was performed, from which global and regional (automatically acquired basal, mid, and apical segments based on LV long-axis length) end-diastolic (EDV) and end-systolic volumes (ESV), LV long-axis length, and sphericity index were obtained.

Results: Global and regional EDV and ESV (indexed to body weight) were most prominently increased in dogs with severe MMVD. All 3 regional LV segments contributed to increased global EDV and ESV with increasing MMVD severity, but mid-EDV contributed the most to the global EDV increase. Furthermore, LV long-axis length and LV sphericity index increased with increasing MMVD severity. Basal and apical EDV segments displayed the strongest association with sphericity index ($P < .0001$).

Conclusions and Clinical Importance: The most prominent LV volume expansion was found in dogs with severe MMVD. Increased EDV, primarily in the mid-segment, leads to rounding of LV apical and basal segments in response to increasing MMVD severity. Assessment of LV volume and shape potentially could allow early detection of dogs at risk for rapid progression into congestive heart failure.

Key words: Cardiology; Echocardiography; Heart failure; Hemodynamics; Valvular disease.

Left ventricular (LV) remodeling in dogs with myxomatous mitral valve disease (MMVD) is characterized by changes in LV geometry in response to chronic volume overload. Normal cardiac output can be maintained for a long period of time, despite increasing mitral regurgitation (MR) by recruitment of cardiac, as well as renal, neurohormonal, and vascular compensatory mechanisms.[1] A major adaptive change to the chronic hemodynamic burden is LV enlargement, and severity of LV enlargement has been shown to be strongly associated with severity of MR in MMVD dogs.[2,3] The enlargement is possible through remodeling of the extracellular matrix with dissolution of collagen weave, allowing rearrangement and slippage of myocardial fibers, and hence LV dilatation.[1,4] As new sarcomeres are added "in series," myocytes are elongated, and the compensatory eccentric hypertrophy normalizes wall stress caused by the volume overload.[4,5] However, the progressively increasing volume overload cannot be indefinitely compensated, and dogs might eventually develop congestive heart failure (CHF).

Assessment of LV geometry is useful when investigating cardiac status and a variety of echocardiographic techniques have been described. Traditional quantitative echocardiographic assessments of the LV used in clinical practice rely on 1-dimensional (M-mode) and 2-dimensional (2D) images. Unfortunately, these assessments can be flawed by assumptions of LV geometry, and by LV foreshortening because of image plane position, potentially leading to inaccuracies in measurements.

Abbreviations:

2D	2-dimensional
CHF	congestive heart failure
EDV	end-diastolic volume
ESV	end-systolic volume
LA/Ao	left atrial to aortic root ratio
LV	left ventricle
LVIDd	end-diastolic left ventricular internal dimension
$LVIDd_{inc}$	percentage increase in end-diastolic left ventricular internal dimension
LVIDs	end-systolic left ventricular internal dimension
$LVIDs_{inc}$	percentage increase in end-systolic left ventricular internal dimension
MMVD	myxomatous mitral valve disease
RT3D	real-time 3-dimensional
SAP	systolic arterial pressure

From the Departments of Clinical Sciences (Ljungvall, Carnabuci, Häggström) and Anatomy, Physiology and Biochemistry (Höglund), Faculty of Veterinary Medicine and Animal Sciences, Swedish University of Agricultural Sciences, Uppsala, Sweden and the Albano Animal Hospital, Danderyd, Sweden (Tidholm). *The study was conducted at the Faculty of Veterinary Medicine and Animal Sciences in Uppsala, Sweden. Abstract accepted for oral research report presentation at the 2011 ACVIM Forum, Denver, CO, USA.*

Corresponding author: I. Ljungvall, Department of Clinical Sciences, Faculty of Veterinary Medicine and Animal Sciences, The Swedish University of Agricultural Sciences, P.O. Box 7054, 75007 Uppsala, Sweden; e-mail: ingrid.ljungvall@slu.se.

Submitted February 1, 2011; Revised May 4, 2011; Accepted June 24, 2011.

10.1111/j.1939-1676.2011.0774.x

These technical limitations can be substantial in diseased hearts when LV geometry is changed.[6,7] Recently, real-time 3-dimensional (RT3D) echocardiographic systems have been introduced. The transducers used in these systems consist of more than 3,000 individual elements, providing superior anatomical delineation of the LV in real time. Furthermore, because of the ability to manipulate the plane to align the true short- and long-axes of the LV, the problems with chamber foreshortening and oblique imaging planes can be reduced, thus providing more anatomically correct apical views than conventional 2D echocardiography.[8,9] The full volume RT3D dataset created from the modeling algorithm can be further divided into 17 regional segments by sectioning from base to apex, perpendicular to the LV long-axis, thereby allowing regional volume assessment.[10]

The LV has been suggested to attain a more globular rather than elliptical shape as LV size increases, as seen in human and canine cardiac diseases of varying etiologies.[11–14] Abnormal changes in LV shape, accompanying the dilating LV, can be assessed by a sphericity index.[13,14] A 3D echocardiographically derived sphericity index has been proven an earlier and more accurate predictor of remodeling compared with other echocardiographic variables after acute myocardial infarction in human patients.[15] Sphericity index usually is not included in the routine echocardiographic protocol when assessing LV remodeling in dogs with cardiac diseases, and sparse information is available regarding the transition into a more globular shape in dogs with naturally acquired MMVD.

By studying the mechanisms of LV remodeling in response to MMVD, important basic concepts of disease progression might be revealed, which might be of value for improved clinical management and prognosis assessment of the individual dog. Hence, the aim of the study was to investigate LV changes in shape and volume in response to different severities of naturally acquired MMVD in dogs by RT3D echocardiography.

Material and Methods

Animals

The study was approved by the Local Ethical Committee in Uppsala, Sweden. Informed owner consent was obtained. Client-owned dogs were prospectively recruited at the cardiology unit of the Faculty of Veterinary Medicine and Animal Sciences in Uppsala. As inclusion criteria for the study, dogs had to either have evidence of MMVD or be free from physical or echocardiographic evidence of cardiac disease. Dogs with congenital heart disease, other acquired cardiovascular disorders, or clinically relevant organ-related or systemic diseases were not included in the study. Dogs in need of heart failure therapy were allowed into the study. Included dogs had to weigh <15 kg.

Procedures

A database was established for each dog, consisting of an owner interview, a physical examination, blood pressure measurement, and an echocardiographic examination, all performed during the same consultation.

All examinations were performed without sedation in a quiet examination room. An owner interview was conducted to collect data concerning age, sex, and medical history. Dogs underwent a general physical examination, and blood pressure was indirectly measured with an automated oscillometric device.[a] Dogs were minimally restrained in a standing position, and an appropriate neonatal cuff, with a width of approximately 40% of the tail circumference, was applied to the base of the tail with the artery marker placed ventrally. Once reliable consecutive readings were obtained, the mean of 5 consecutive blood pressure measurements was calculated.

Echocardiographic examinations, which included M-mode, 2D, and RT3D examinations, were performed by use of an ultrasonographic unit[b] equipped with a 5-1 MHz transducer (for M-mode and 2D), a 7-2 MHz matrix transducer (for 2D and RT3D), and ECG monitoring. The echocardiographic examinations all were performed and evaluated by the same echocardiographer (I.L.). Dogs were gently restrained in right and left lateral recumbency on an ultrasound examination table.

M-mode and 2D Data

Standardized M-mode and 2D loops[16] were digitally stored. Assessment of mitral valve structures was conducted from right parasternal long-axis views and left apical 4-chamber view. The same views were used to assess the degree of MR by color Doppler mapping. MR was subjectively assessed as the area of regurgitant jet relative to the area of the left atrium, as described elsewhere[17] with slight modifications according to the following: regurgitation scores were recorded as none, mild ($<30\%$), moderate (>30–50%), and severe ($>50\%$). The left atrial to aortic root (LA/Ao) ratio was measured as described previously.[18] Measurements were made on 3 consecutive cardiac cycles and the mean value from each dog was used in the statistical analysis. Screening of potential regurgitations through the tricuspid, aortic, and pulmonic valves was performed routinely by color Doppler echocardiography. M-mode measurements of the LV were performed by standard techniques[19] on images obtained from the right parasternal short-axis view on 5 consecutive cardiac cycles. The mean value for each variable was used in the statistical analyses. Values for the percent increases of end-diastolic left ventricular internal dimension ($LVIDd_{inc}$) and end-systolic left ventricular internal dimension ($LVIDs_{inc}$) were calculated as follows: [observed dimension−expected normal dimension]/expected normal dimension $\times$ 100. Expected normal dimensions were calculated as previously described: LVIDd (body weight$^{0.294}$ $\times$ 1.53) and LVIDs (body weight$^{0.315}$ $\times$ 0.95) (Table 1).[20]

Diagnosis of MMVD was exclusively based on color Doppler and 2D echocardiographic findings, and diagnostic criteria included characteristic valvular lesions of the mitral valve apparatus (thickened or prolapsing mitral valve leaflets or both) and demonstrated MR on color Doppler echocardiogram, as described previously.[17,21] Estimation of MMVD severity was based on the obtained LA/Ao ratio and the MR jet size, and dogs were classified as follows: healthy (LA/Ao <1.5 and none to minimal MR jet), mild (LA/Ao ≤ 1.5 and MR jet $\leq 30\%$), moderate (LA/Ao >1.5 and <1.8 and MR jet >30–50%), and severe (LA/Ao ≥ 1.8 and MR jet $>50\%$).

RT3D Data

The RT3D dataset was acquired from the left parasternal apical 4-chamber view. The lowest possible scan line density was used to produce the largest possible pyramidal volume of acquisition. Series of 4–7 consecutive ECG R-wave triggered cycles were acquired, from which 4 subvolumes were automatically derived and integrated into 1 pyramidal volume, thereby providing a RT3D full-volume dataset of the entire LV. Quality control of the dataset was performed immediately after data collection, and resampling was

Table 1. Summary of dog characteristics, clinical, and echocardiographic data in healthy dogs (n = 20) and dogs in various stages of MMVD (n = 45).

Group	Healthy	Mild	Moderate	Severe
Number	20	20	8	17
Sex (female/male)	16/4	14/6	4/4	5/12
CKCS (yes/no)	16/4	17/3	5/3	9/8
Age (years)	4.9 (2.8–6.4)[b]	6.9 (6.0–10)[b]	8.5 (7.0–9.6)[b]	9.4 (8.7–11)[b]
Weight (kg)	8.0 (7.0–9.9)[a,b]	9.4(7.8–11)[a]	10 (7.6–11)[a,b]	10 (7.8–12)[b]
HR (bpm)	108 (99–121)[a]	104 (92–125)[a,b]	107 (101–142)[a,b]	136 (120–163)[b]
SAP (mmHg)	134 (119–138)[a]	138 (130–148)[a,b]	144 (133–154)[a,b]	124 (116–137)[a,c]
LA/Ao	1.2 (1.1–1.2)[a]	1.3 (1.2–1.4)[b]	1.6 (1.5–1.6)[b,c]	2.1 (2.0–2.6)[d]
LVIDd (cm)	2.9 (2.7–3.3)[a]	3.3 (3-1-3.6)[a,b]	3.7 (3.4–4.5)[b]	4.3 (4.1–4.8)[b,c]
$LVIDd_{inc}$ (%)	4.0 (−3.8–14)[a]	11(3.7–23)[a,b]	27 (19–45)[b,c]	44 (40–59)[c]
LVIDs (cm)	2.0 (1.8-2-4)[a]	2.3 (2.0–2.6)[a]	2.4 (2.2–3.0)[a,b]	2.7 (2.5–3.2)[b]
$LVIDs_{inc}$ (%)	6.1 (−0.2–28)[a]	18 (11–29)[a]	24 (17–51)[a,b]	43 (26–56)[b]
FS (%)	32 (27–34)[a]	30 (26–34)[a]	35 (32–37)[a,b]	36 (31–41)[b]
RT3D global EDV/kg	2.3 (2.1–2.8)[a]	2.5 (2.3–2.8)[a]	2.8 (2.5–3.2)[a]	4.0 (3.7–4.5)[b]
RT3D basal EDV/kg (mL)	0.9 (0.8–1.1)[a]	0.9 (0.8–1.0)[a]	0.9 (0.8–1.2)[a]	1.5 (1.3–1.7)[b]
RT3D mid EDV/kg (mL)	0.9 (0.8–1.1)[a]	0.9 (0.9–1.0)[a]	1.1 (1.0–1.3)[a]	1.6 (1.4–1.7)[b]
RT3D apical EDV/kg (mL)	0.5 (0.5–0.7)[a]	0.6 (0.6–0.7)[a]	0.7 (0.6–0.8)[a]	1 (0.9–1.1)[b]
RT3D global ESV/kg	1.2 (1.1–1.6)[a]	1.3 (1.2–1.6)[a]	1.4 (1.2–1.5)[a]	1.7 (1.5–2.2)[b]
RT3D basal ESV/kg (mL)	0.5 (0.4–0.6)[a]	0.5 (0.5–0.6)[a]	0.5 (0.4–0.6)[a,b]	0.6 (0.6–0.9)[b]
RT3D mid ESV/kg (mL)	0.4 (0.4–0.6)[a]	0.5 (0.4–0.6)[a]	0.5 (0.4–0.6)[a,b]	0.6 (0.5–0.8)[b]
RT3D apical ESV/kg (mL)	0.3 (0.3–0.4)[a]	0.3 (0.3–0.4)[a]	0.3 (0.3–0.4)[a]	0.4 (0.4–0.5)[b]
RT3D basal EDV(%)	37.7 (36 –41.4)[a]	37.7 (36–38.4)[a]	35.6 (31.5–37.6)[a]	35.9 (35.1–37.6)[a]
RT3D mid EDV(%)	38.3 (36.7–39.8)[a,b]	37.8 (36.4–38.3)[a]	40.5 (38.8–41.1)[b]	38.9 (37.4–40.2)[a,b]
RT3D apical EDV(%)	23.2 (20.7–25.5)[a]	25 (23.7–26.8)[a]	24.1 (22.4–28.9)[a]	24.6 (23.6–26.5)[a]
RT3D basal ESV(%)	39.8 (37.6–43.3)[a]	40.2 (38.5–42.5)[a]	39.2 (36.8–41)[a]	39.5 (36.6–42)[a]
RT3D mid ESV(%)	36 (34.5–37.6)[a]	36 (34.2–38.1)[a]	35.4 (34.6–37.5)[a]	36.1 (33.7-37-5)[a]
RT3D apical ESV(%)	23 (21.9–27.2)[a]	23.2 (21.2–25.6)[a]	24.4 (21.5–28.8)[a]	23.9 (21.9–28.8)[a]
RT3D EF (%)	46 (44–50)[a]	48 (44–50)[a]	53 (48–54)[a,b]	56 (50–61)[b]
RT3D sphericity	0.8 (0.7–1)[a]	0.9 (0.7–1)[a]	1 (0.8–1.2)[a,b]	1.2 (0.9–1.2)[b]
RT3D long-axis length (cm)	3.6 (3.4–4.3)[a]	3.6 (3.5–3.9)[a]	3.8 (3.5–4.1)[a]	4.1 (3.8–4.4)[b]

Values are reported as median and interquartile ranges (IQR). Within each row, values with different superscript letter are significantly ($P > .008$) different.

HR, heart rate; SAP, systolic arterial pressure, basic echocardiographic data; LA/Ao, ratio of left atrium to aortic root; $LVIDd_{inc}$, percentage increase in end-diastolic left ventricular internal dimension; $LVIDs_{inc}$, percentage increase in end-systolic left ventricular internal dimension; FS, fractional shortening; RT3D, real-time 3-dimensional; EDV/kg and ESV/kg, global-, basal-, mid-, and apical end-diastolic and end-systolic volumes indexed to body weight; basal, mid, and apical EDV% and ESV%, percentage contribution to the global EDV and ESV of each segment; EF, ejection fraction.

performed in cases of suboptimal image quality or poor definition of LV cavity.

The RT3D data analyses were performed off-line by commercial software.[c] The software displays the RT3D volume data in 3 different orthogonal planes: the 2- and 4-chamber views, and the short-axis view. The orthogonal planes all were aligned interactively by use of color-coded conventions, according to the manufacturer's instructions, in order to obtain the most anatomically correct apical views for optimal border delineation of the LV. Simplified, orientation of the 2- and 4-chamber long-axes views were determined by positioning color-coded lines along the LV long axes before positioning lines at the mid-papillary level perpendicular to the long axes. Position of the lines, determined previously in the LV long-axes views, were optimized in the short-axis view. In order to prevent foreshortening of the LV, care was taken to include the largest long-axis dimension, and to exclude the aortic outflow tract in the view. The data loop then was played in order to check for accuracy of all frames in the loop, and readjustments were performed when required. Once the LV axes were appropriately aligned, a semiautomatic endocardial border detection process was started in each plane for assessment of end-diastolic (EDV) and end-systolic (ESV) LV volumes. All voxels (ie, the volume elements representing intensity of echocardiographic reflections at a particular point in space) were used in the border detection process. The end-diastolic frame was identical to the 1st frame in the loop on the RT3D dataset, corresponding to the peak of the R wave on the ECG. Five anatomic landmarks were manually defined at the endocardial border in the LV cavity: 2 reference points at the mitral annulus hinge points in each of the 4- and 2-chamber views, and 1 reference point at the apex in the 4-chamber view. The endocardial border then was traced by an automated detection process to create a cast of the LV cavity. In each view, the border detection of the LV cavity was verified for accuracy, and the endocardial borders including papillary muscles were manually adjusted as required. Subsequently, the end-systolic frame was selected, identified as the frame preceding mitral valve opening. Anatomic landmarks definition, automatic endocardial border detection, and manual adjustment of border detection were repeated on this frame as described for the end-diastolic frame. In order to further control the border detection accuracy of the LV cavity, careful frame-by-frame assessment was performed during the entire cardiac cycle. The traced borders then were processed to automatically calculate the EDV and ESV by the software (Fig 1). Both EDV and ESV were indexed to body weight (EDV/kg and ESV/kg). The RT3D long-axis length was measured in the 4-chamber view as the distance from the endocardial apex to the mid-point of the mitral valve.

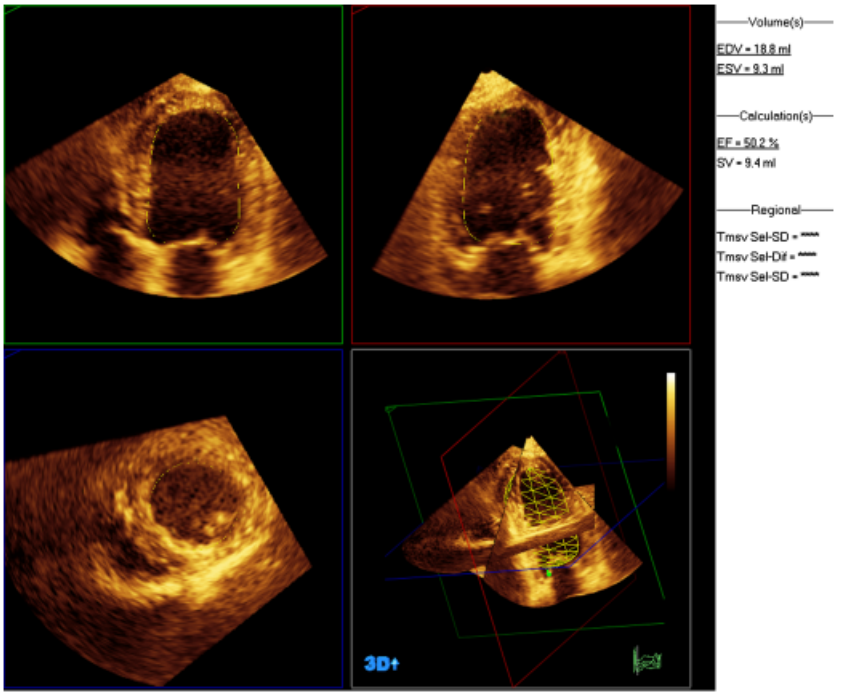

Fig 1. Example of a real-time 3-dimensional volume dataset displayed in 3 orthogonal planes; the 2- and 4-chamber views, and the short-axis view, from which endocardial borders of the LV cast were identified, and end-diastolic and end-systolic LV volumes were obtained.

Seventeen segments, defined by the American Society of Echocardiography,[10] were automatically calculated from the LV cast, allowing regional RT3D LV volume assessment (Fig 2). The different segments were identified on the LV cast as fractions of the LV long-axis length. The 17 segments were further joined into 3 major segments: basal EDV and ESV included segments 1–6, mid-EDV and ESV included segments 7–12 and apical EDV, and ESV included segments 13–17. The 17-segment model creates a distribution of 30, 35, and 35%, respectively, for the basal, mid, and apical portions of the LV long-axis length, according to the manufacturer of the software. Percentage contribution to the global EDV and ESV of each of the major regional segments was calculated (basal, mid, and apical EDV% and ESV%). Sphericity index was calculated as the RT3D-EDV divided by the volume of a sphere, whereby the sphere volume was calculated as $1/6\pi \times L^3$ (where L is equal to the LV long-axis length).[14]

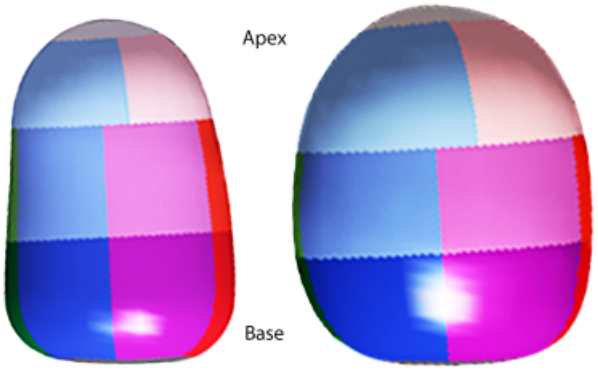

Fig 2. Left ventricular casts obtained from the real-time 3-dimensional dataset from a healthy dog (left) and a dog with severe myxomatous mitral valve disease (MMVD) (right). The left ventricular (LV) casts were automatically segmented into 17 segments. The LV sphericity index increased with increasing MMVD severity, indicating that the LV shape changes from elliptical to more globular in response to chronic volume overload.

Assessment of Variability

The intraobserver acquisition and measurement variability of the RT3D global and regional volume data was tested in 5 dogs. Repeated image acquisition was performed in each dog at 3 different time points on a given day. One RT3D image from each of the time points was selected for global and regional EDV and ESV measurement (>5 hours between measurements of the 3 dataset from each dog). The resulting mean values and standard deviations were used to determine the coefficient of variation (CV). Global EDV had a median value of 1.3%, and global ESV had a median value of 3.8%. All regional EDV and ESV segments had median CV values below 12%.

Statistical Analyses

Commercially available software[d] was used for all statistical analyses. Data are presented as medians and interquartile ranges (IQR). A value of $P < .05$ was considered significant for the analyses, unless otherwise indicated. Global and regional EDV and ESV values indexed to body weight (EDV/kg and ESV/kg) were used in the statistical analysis.

The nonparametric Kruskal-Wallis test was used to investigate overall differences among the 4 MMVD severity groups, and global and regional EDV and ESV, regional EDV% and ESV%, long-axis length, and sphericity index. If a significant difference was detected, a pair-wise comparison also was performed by use of the Mann-Whitney U-test with Bonferroni's adjustment, for which a value of $P < .008$ was considered significant. In addition, a comparison was performed including only dogs with severe MMVD, with or without CHF.

Univariable regression analyses were used to evaluate associations between global and regional EDV and ESV, regional EDV%

and ESV%, long-axis length, sphericity index, and systolic arterial pressure (SAP), and the echocardiographic M-mode and 2D measurements: LA/Ao ratio, $LVIDd_{inc}$, $LVIDs_{inc}$. Furthermore, potential associations between the sphericity index, and global and regional EDV and ESV, and regional EDV% and ESV%, also were investigated.

Results

A total of 65 dogs (28 females and 37 males) with a median age of 7.6 (IQR 5.7–9.6) years and a median body weight of 9.4 (IQR 7.6–10.6) kg were included in the study. Twenty dogs had unremarkable echocardiograms and were considered healthy, 20 dogs had mild MMVD, 8 dogs had moderate MMVD, and 17 dogs had severe MMVD. Eleven of the severe MMVD dogs were diagnosed with CHF at the time of inclusion or had been diagnosed previously with CHF but stabilized by heart failure therapy. Nine of these dogs were receiving cardiac medications: furosemide (9 dogs), pimobendan (7 dogs), ACE inhibitor (5 dogs), spironolactone (1 dog), and digoxin (3 dogs). The most commonly recruited breed was Cavalier King Charles Spaniel (n = 47), followed by Dachshund (n = 7), mixed breed (n = 3), and Jack Russell (n = 2). Six other breeds with 1 dog each also were represented in the study.

Group-Wise Comparisons

Overall significant differences were found among the 4 MMVD severity groups and global EDV, basal EDV, mid-EDV, apical EDV (all $P < .0001$), global ESV ($P = .0006$), basal ESV ($P = .0061$), mid-ESV ($P = .0033$), apical ESV ($P = .0003$), basal EDV% ($P = .039$), mid-EDV% ($P = .024$), long-axis length ($P = .0007$), and sphericity index ($P = .0008$).

Dogs with severe MMVD had higher values of EDV compared with values in healthy dogs and dogs with mild (global EDV, basal EDV, mid-EDV, and apical EDV; all $P < .0001$) and moderate (global EDV; $P = .0003$, basal EDV; $P = .0005$; mid-EDV; $P = .0005$, apical EDV; $P = .0002$) MMVD. Additionally, dogs with severe MMVD had higher values of ESV compared with values in healthy dogs (global ESV; $P = .0003$, basal ESV; $P = .0031$, mid-ESV; $P = .0014$, apical ESV; $P = .0003$) and dogs with mild (global ESV; $P = .0011$, basal ESV; $P = .0042$, mid-ESV; $P = .0042$, apical ESV; $P = .0003$) and moderate (global ESV; $P = .0036$, apical ESV; $P = .0043$) MMVD. Dogs with moderate MMVD had higher mid-EDV% compared with values in dogs with mild MMVD ($P = .007$).

Dogs with severe MMVD had higher values of long-axis length compared with values in healthy dogs ($P = .0009$) and dogs with mild ($P = .0004$) and moderate ($P = .0074$) MMVD. Dogs with severe MMVD had higher values of sphericity index compared with values in healthy dogs ($P = .0011$) and dogs with mild ($P = .0016$) MMVD (Fig 2).

The apical EDV% was higher in severe MMVD dogs diagnosed with CHF compared with severe MMVD dogs without CHF ($P = .0067$).

Regression Analyses

Global EDV, basal EDV, mid-EDV, and apical EDV increased with increasing LA/Ao ratio ($R^2 = 0.61$, 0.56, 0.59, and 0.59, respectively, all $P < .0001$), $LVIDd_{inc}$ ($R^2 = 0.61$, 0.54, 0.62, and 0.58, respectively, all $P < .0001$), and $LVIDs_{inc}$ ($R^2 = 0.41$, 0.37, 0.42, and 0.38, respectively, all $P < .0001$), and with decreasing SAP (global EDV; $R^2 = 0.13$, $P = .002$, basal EDV; $R^2 = 0.13$, $P = .0032$, mid-EDV; $R^2 = 0.14$, $P = .0021$, and apical EDV; $R^2 = 0.13$, $P = .0027$). Basal EDV% decreased with increasing $LVIDd_{inc}$ ($R^2 = 0.06$, $P = .05$), and mid-EDV% increased with increasing $LVIDd_{inc}$ ($R^2 = 0.06$, $P = .048$). Furthermore, global ESV, basal ESV, mid-ESV, and apical ESV increased with increasing LA/Ao ratio ($R^2 = 0.27$, 0.25, 0.22, and 0.29, respectively, all $P < .0001$), $LVIDd_{inc}$ ($R^2 = 0.32$, 0.28, 0.28, and 0.34, respectively, all $P < .0001$), $LVIDs_{inc}$ ($R^2 = 0.26$, 0.25, 0.24, and 0.22, respectively, all $P < .0001$), and with decreasing SAP (global ESV; $R^2 = 0.12$, $P = .0038$, basal ESV; $R^2 = 0.09$, $P = .018$, mid-ESV; $R^2 = 0.13$, $P = .0037$, and apical ESV; $R^2 = 0.15$, $P = .0017$). Mid-ESV% increased with increasing global ESV ($R^2 = 0.08$, $P = .019$).

Long-axis length increased with increasing LA/Ao ($R^2 = 0.11$, $P = .0077$), $LVIDd_{inc}$ ($R^2 = 0.18$, $P = .0005$), $LVIDs_{inc}$ ($R^2 = 0.20$, $P = .0002$). Sphericity index increased with increasing LA/Ao ($R^2 = 0.27$, $P < .0001$), $LVIDd_{inc}$ ($R^2 = 0.25$, $P < .0001$), $LVIDs_{inc}$ ($R^2 = 0.11$, $P = .0064$), global EDV ($R^2 = 0.21$, $P = .0002$), basal EDV ($R^2 = 0.11$, $P = .0069$) mid-EDV ($R^2 = 0.21$, $P = .0002$), apical EDV ($R^2 = 0.34$, $P < .0001$), global ESV ($R^2 = 0.09$, $P = .017$), apical ESV ($R^2 = 0.20$, $P = .0002$). Finally, sphericity index increased with decreasing basal EDV% ($R^2 = 0.33$, $P < .0001$) and with increasing apical EDV% ($R^2 = 0.31$, $P < .0001$), mid-ESV% ($R^2 = 0.09$, $P = .018$), and apical ESV% ($R^2 = 0.13$, $P = .0034$) (Fig 3).

Discussion

The present RT3D echocardiographic study showed prominent LV volume expansion only in dogs with more severe MMVD. All 3 regional LV segments contributed to the increase in global EDV and ESV with increasing MMVD severity, but mid-EDV contributed the most to the global EDV increase. The increase in LV sphericity index with increasing disease severity indicates that the LV shape changes from elliptical to more globular in response to chronic volume overload. The apical and basal segments contributed the most to the increased sphericity.

Group-wise comparisons of global and regional EDV and ESV, using a conservative P-value ($< .008$), only separated dogs with severe MMVD from other MMVD severity groups. This result is in accordance with a previous study by radiography, M-mode, and 2D echocardiography to investigate the course of enlargement of left heart chambers before onset of CHF in dogs with MMVD.[22] Left heart chamber enlargement was characterized by a slow phase of steadily progressing MMVD until about 6–12 months before onset of CHF,

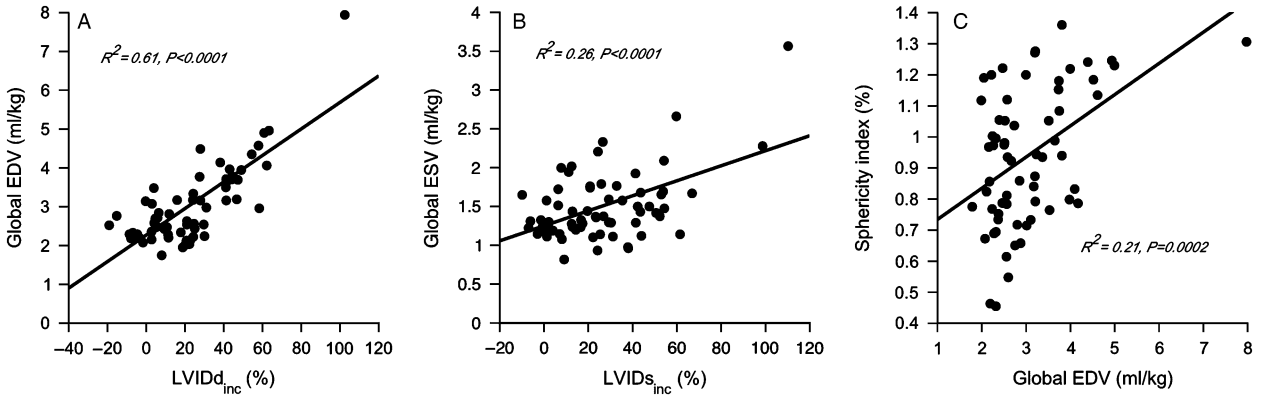

Fig 3. Associations between (A) percentage increase in end-diastolic left ventricular internal dimension (LVIDd$_{inc}$%) and global end-diastolic volume indexed to body weight (EDV/kg), (B) percentage increase in end-systolic left ventricular internal dimension (LVIDs$_{inc}$%) and global end-systolic volume indexed to body weight (global ESV/kg), and (C) global EDV/kg and sphericity index; in 65 dogs with or without myxomatous mitral valve disease.

when rate of change of enlargement was fast. Also, circulating B-type natriuretic peptide in dogs with MMVD has been shown to increase more drastically in late stages of the disease, reflecting more pronounced LV myocardial stretch because of severe volume overload in dogs with imminent CHF.[23] Combining various diagnostic methods might improve prediction of outcome for dogs with MMVD. The design of the present study did not include longitudinal follow-up of individual dogs, hence assessment of volume increase until manifestation of decompensated CHF could not be performed. However, the results clearly suggest that the greatest volume increase occurs in the more severe stage of MMVD. Based on this finding, routinely performed volume assessment potentially could improve prediction of outcome for the individual dog, thus allowing detection of risk of forthcoming CHF at an earlier stage. However, in order to use RT3D LV volumes in clinical practice, normal reference values need to be established. Although clinical use of modern 3D systems is facilitated by advances in computer technology, reducing acquisition and postprocessing time, a shortcoming of the RT3D technique still lies in the fact that it is more time consuming compared with more traditional echocardiographic techniques.

The LV mid-segment was the segment contributing the most to the global increase in EDV and ESV in comparison with the other segments, according to both group-wise comparisons and linear regression analyses. However, these linear regression associations were weak. Potentially, LV anatomy allows more pronounced myocardial stretch in the mid-segment, whereas the apical and basal segments are more restricted to LV expansion, because of supporting structures such as the AV annular ring in the basal segment. In addition, the LV has a smaller diameter in the apical region than in the mid-segment, and because pressure within the LV at a given moment is the same, regardless location, the wall stress is smaller in the apical than in the mid-segment, according to LaPlace's law. This, in turn, leads to lesser tendency for dilatation of the apex. The percentage contribution of mid-segment to global EDV was only significantly higher in dogs with moderate MMVD compared with values in dogs with mild MMVD. Hence, according to this result, the mid-segment is more likely to dilate at an earlier timepoint, compared with the other segments.

The results from the present study support the recommendation that the mid-segment is more appropriate than the basal and apical segments for M-mode measurement of LV dimensions. LV volume estimation using M-mode derived LV dimensions, are based on the assumption that LV is a prolate ellipsoid, and that volume can be calculated by measuring a single minor-axis dimension and cubing it. Hence, converting linear measurement of the LV to a 3D volume might result in inaccuracies, especially in the dilated, spherical LV encountered because of chronic volume overload.[24,25] In contrast, volume assessment by RT3D makes no assumption about LV shape because of the modeling algorithm used in the software.

LV geometry was further assessed by the sphericity index, which addresses global changes in the LV shape. In the present study, LV sphericity index increased with increasing MMVD severity, indicating that the LV shape changes from elliptical to more globular in response to chronic volume overload. The sphericity index has been reported to indirectly measure the degree of mitral leaflet tethering in human cardiac patients and in experimentally induced cardiac disease in dogs, because increasing LV sphericity causes apical and lateral papillary muscle displacement and disruption of normal mitral annular geometry, resulting in secondary MR and aggravated left-sided volume overload.[26–28] Furthermore, alterations in spherical geometry might influence LV apical rotation and twist, which has been proven of fundamental importance for systolic function.[29,30] Assessing regional contribution to changes in LV shape, sphericity index was associated with decreasing percentage contribution of basal EDV to global EDV and increasing percentage of apical EDV. Likely, this reflects that the theoretical sphere excludes the peripheral part of the LV base in dogs with more normal elliptical LV. Rounding of the LV base with increasing MMVD severity results in a better fit of the basal EDV into the sphere, and this change in LV shape leads to a decreased volume

percentage of the global EDV. The apical EDV segment in the elliptical LV has less contact with the theoretical sphere, compared with in the spherical LV, which results in increased percentage apical EDV with increasing sphericity index. Although the mid-segment was increasing the most with increasing volume overload, no association was shown between sphericity index and percentage contribution of mid-EDV to the global EDV, most likely reflecting that only minor changes occur in the LV mid-segmental shape with increasing MMVD severity. These findings, in combination with the result that the long-axis length increased with increasing disease severity, suggest that although the LV changes into a more globular shape with increasing MMVD severity, the final shape is not an absolute sphere (Fig 2).

Interpretation of changes in LV volume, shape, and function is complex because they all might influence each other. In dogs with MMVD, forward stroke volume is known to decrease during disease progression[31] as a consequence of chronic volume overload and low resistance to ventricular empting into the left atrium. Dogs with severe MR because of MMVD might eject $>75\%$ of the total stroke volume into the left atrium.[3] This potentially could explain the decrease in SAP with increasing EDV and ESV. Furthermore, SAP was lower in dogs with severe MMVD compared with values in dogs with other disease severities. The results suggest that the decreased forward stroke volume is ultimately difficult to compensate completely, resulting in decreased SAP in dogs with volume overload associated with severe MMVD. However, all dogs had SAP within, or close to, normal reference ranges, indicating that the LV forward systolic function does not decline dramatically, and that regulatory mechanisms contribute to maintenance of acceptable SAP even in the severe stage of the disease.

There are some limitations to the study; the lack of dependence on geometric modeling and image plane positioning by RT3D echocardiography should theoretically result in accurate chamber quantification.[8] Because of lack of evaluation of the RT3D volume assessments against a gold standard technique, such as magnetic resonance imaging, this statement could not be evaluated. However, the present study did not aim to investigate the accuracy of RT3D echocardiography for volume assessment in dogs, but rather to investigate potential geometrical and volumetric differences among dogs with different severities of MMVD. RT3D echocardiographic images can suffer from poor image quality by the same causes as 2D images. Motion disturbances caused by movements of the dog or by respiratory movements, including lung interference, or by pronounced sinus arrhythmia, all might cause problems constructing a full-volume image of acceptable quality. All RT3D images were checked for sufficient quality immediately after sampling, and resampling was performed in cases of suboptimal image quality or poor definition of LV cavity. Although images were of variable quality, RT3D images from all dogs were of sufficient quality to obtain the required information and no dog was excluded because of poor acoustic window.

In conclusion, this RT3D echocardiography study showed that chronic volume overload in dogs with MMVD leads to abnormal geometry of the LV, which increased in size and sphericity with increasing disease severity. However, a prominent LV volume expansion was only found in dogs with more severe MMVD. The mid-EDV contributed the most to the global EDV increase. The LV shape changed from elliptical to more globular in response to increasing volume overload, with the basal and apical segments contributing the most to the increase in sphericity. Routine assessment of LV volume and shape potentially could lead to earlier detection of dogs at risk for rapid progression into CHF. However, longitudinal follow-up studies are needed to investigate whether RT3D echocardiography could improve prediction of outcome in dogs with MMVD.

Footnotes

[a] Vet HDO monitor, S+B medVet GmbH, Babenhausen, Germany
[b] iE33, Philips Ultrasound, Bothell, WA
[c] QLAB advanced quantification, version 7.0, Philips Ultrasound
[d] JMP, version 8.0.1, SAS Institute Inc, Cary, NC

Acknowledgment

The technical assistance from Philips Ultrasound system, Sweden is greatly appreciated.

References

1. Dell'italia LJ, Balcells E, Meng QC, et al. Volume-overload cardiac hypertrophy is unaffected by ACE inhibitor treatment in dogs. Am J Physiol 1997;273:H961–H970.

2. Häggstrom J, Hansson K, Karlberg B, et al. Plasma concentration of atrial natriuretic peptide in relation to severity of mitral regurgitation in Cavalier King Charles Spaniels. Am J Vet Res 1994;55:698–703.

3. Kittleson M, Brown W. Regurgitant fraction measured by using the proximal isovelocity surface area method in dogs with chronic myxomatous mitral valve disease. J Vet Intern Med 2003;17:84–88.

4. Grossman W, Jones D, McLaurin LP. Wall stress and patterns of hypertrophy in the human left ventricle. J Clin Invest 1975;56:56–64.

5. Carabello BA. Concentric versus eccentric remodeling. J Card Fail 2002;8:S258–S263.

6. Kupferwasser I, Mohr-Kahaly S, Stahr P, et al. Transthoracic three-dimensional echocardiographic volumetry of distorted left ventricles using rotational scanning. J Am Soc Echocardiogr 1997;10:840–852.

7. Lang RM, Bierig M, Devereux RB, et al. Recommendations for chamber quantification: A report from the American Society of Echocardiography's Guidelines and Standards Committee and the Chamber Quantification Writing Group, developed in conjunction with the European Association of Echocardiography, a branch of the European Society of Cardiology. J Am Soc Echocardiogr 2005;18:1440–1463.

8. Lang RM, Mor-Avi V, Sugeng L, et al. Three-dimensional echocardiography: The benefits of the additional dimension. J Am Coll Cardiol 2006;48:2053–2069.

9. Jacobs LD, Salgo IS, Goonewardena S, et al. Rapid online quantification of left ventricular volume from real-time three-dimensional echocardiographic data. Eur Heart J 2006;27: 460–468.

10. Cerqueira MD, Weissman NJ, Dilsizian V, et al. Standardized myocardial segmentation and nomenclature for tomographic imaging of the heart: A statement for healthcare professionals from the Cardiac Imaging Committee of the Council on Clinical Cardiology of the American Heart Association. Circulation 2002;105: 539–542.

11. Lord PF. Left ventricular volumes of diseased canine heart: Congestive cardiomyopathy and volume overload (patent ductus arteriosus and primary mitral valvular insufficiency). Am J Vet Res 1974;35:493–501.

12. Young AA, Orr R, Smaill BH, et al. Three-dimensional changes in left and right ventricular geometry in chronic mitral regurgitation. Am J Physiol 1996;271:H2689–H2700.

13. Monaghan MJ. Role of real time 3D echocardiography in evaluating the left ventricle. Heart 2006;92:131–136.

14. Di Donato M, Dabic P, Castelvecchio S, et al. Left ventricular geometry in normal and post-anterior myocardial infarction patients: Sphericity index and 'new' conicity index comparisons. Eur J Cardiothorac Surg 2006;29(Suppl 1):S225–S230.

15. Mannaerts HF, van der Heide JA, Kamp O, et al. Early identification of left ventricular remodelling after myocardial infarction, assessed by transthoracic 3D echocardiography. Eur Heart J 2004;25:680–687.

16. Thomas W, Gaber C, Jacobs G, et al. Recommendations for standards in transthoracic two-dimensional echocardiography in the dog and cat. Echocardiography Committee of the Specialty of Cardiology, American College of Veterinary Internal Medicine. J Vet Intern Med 1993;7:247–252.

17. Olsen L, Martinussen T, Pedersen HD. Early echocardiographic predictors of myxomatous mitral valve disease in Dachshunds. Vet Rec 2003;152:293–297.

18. Hansson K, Haggstrom J, Kvart C, et al. Left atrial to aortic root indices using two-dimensional and M-mode echocardiography in Cavalier King Charles Spaniels with and without left atrial enlargement. Vet Radiol Ultrasound 2002;43:568–575.

19. Bélanger MC. Echocardiography. In: Ettinger SJ, Feldman EC, eds. Textbook of Veterinary Internal Medicine, 6th ed. St Louis, MO: Elsevier Saunders; 2005:311–326.

20. Cornell C, Kittleson M, Della Torre P, et al. Allometric scaling of M-mode cardiac measurements in normal adult dogs. J Vet Intern Med 2004;18:311–321.

21. Pedersen HD, Kristensen B, Norby B, et al. Echocardiographic study of mitral valve prolapse in Dachshunds. Zentralbl Veterinarmed A 1996;43:103–110.

22. Lord P, Hansson K, Kvart C, et al. Rate of change of heart size before congestive heart failure in dogs with mitral regurgitation. J Small Anim Pract 2010;51:210–218.

23. Tarnow I, Olsen LH, Kvart C, et al. Predictive value of natriuretic peptides in dogs with mitral valve disease. Vet J 2009;180:195–201.

24. Teichholz LE, Kreulen T, Herman MV, et al. Problems in echocardiographic volume determinations: Echocardiographic-angiographic correlations in the presence of absence of asynergy. Am J Cardiol 1976;37:7–11.

25. Tidholm A, Westling AB, Höglund K, et al. Comparisons of 3-, 2-dimensional, and M-mode echocardiographical methods for estimation of left chamber volumes in dogs with and without acquired heart disease. J Vet Intern Med 2010;24:1414–1420.

26. Otsuji Y, Handschumacher MD, Schwammenthal E, et al. Insights from three-dimensional echocardiography into the mechanism of functional mitral regurgitation: Direct in vivo demonstration of altered leaflet tethering geometry. Circulation 1997;96: 1999–2008.

27. Lapu-Bula R, Robert A, Van Craeynest D, et al. Contribution of exercise-induced mitral regurgitation to exercise stroke volume and exercise capacity in patients with left ventricular systolic dysfunction. Circulation 2002;106:1342–1348.

28. Hung J, Papakostas L, Tahta SA, et al. Mechanism of recurrent ischemic mitral regurgitation after annuloplasty: Continued LV remodeling as a moving target. Circulation 2004;110:II85–90.

29. Sengupta PP, Tajik AJ, Chandrasekaran K, et al. Twist mechanics of the left ventricle: Principles and application. JACC Cardiovasc Imag 2008;1:366–376.

30. van Dalen BM, Kauer F, Vletter WB, et al. Influence of cardiac shape on left ventricular twist. J Appl Physiol 2010;108: 146–151.

31. Borgarelli M, Tarducci A, Zanatta R, et al. Decreased systolic function and inadequate hypertrophy in large and small breed dogs with chronic mitral valve insufficiency. J Vet Intern Med 2007;21:61–67.